Solar Cells

A. Ghicov, S. P. Albu, R. Hahn, D. Kim, T. Stergiopoulos, J. Kunze, C.-A. Schiller, P. Falaras, P. Schmuki*

TiO_2 Nanotubes in Dye-Sensitized Solar Cells: Critical Factors for the Conversion Efficiency

Particle vs tube: The present paper systematically investigates a range of fundamental geometrical and structural features of TiO_2 nanotube layers and their effect on the dye-sensitized solar cell conversion efficiency, to deduce the most promising strategies for improvement. It is found that the performance of the cells strongly depends on the morphology and crystalline structure of the nanotubes.

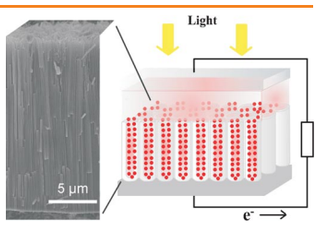

Chem. Asian J.
DOI: **10.1002/asia.200800441**

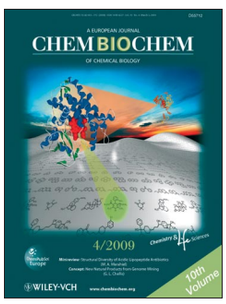

Protein Aggregation

A. Taniguchi, Y. Sohma, Y. Hirayama, H. Mukai, T. Kimura, Y. Hayashi, K. Matsuzaki, Y. Kiso*

"Click Peptide": pH-Triggered in Situ Production and Aggregation of Monomer Aβ1–42

Into neutral: We demonstrate the unique features of a pH click peptide based on an O-acyl isopeptide method. Under acidic conditions, the click peptide remains in a monomeric form. Upon increase of the pH to 7.4, the click peptide is quickly able to convert into Aβ1–42 through an O-to-N intramolecular acyl migration. Further study using this pH click peptide would elucidate the pathological role of Aβ1–42 in Alzheimer's disease.

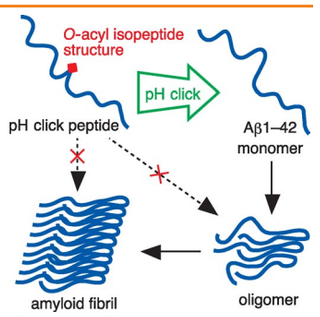

ChemBioChem
DOI: **10.1002/cbic.200800765**

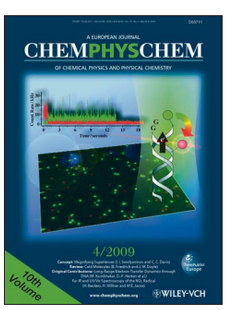

Carbon Nanotubes

P. Gründler,* O. Frank, L. Kavan, L. Dunsch

Carbon Nanotube Electrodes for Hot-Wire Electrochemistry

Hot-wired electrodes: Thin metallic wires ($d = 25$ µm) are covered with a 3 µm layer of single-walled carbon nanotubes (SWCNTs; see image) by electrophoresis from a suspension containing excess ionic surfactant. A pure SWCNT surface is achieved by heating the electrode in air. Strong differences between covered and bare metallic electrodes occur with in situ heating during electrochemical experiments.

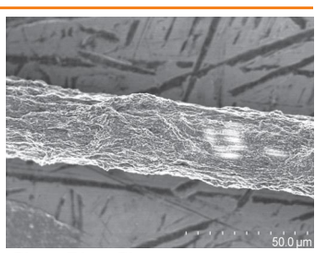

ChemPhysChem
DOI: **10.1002/cphc.200800659**

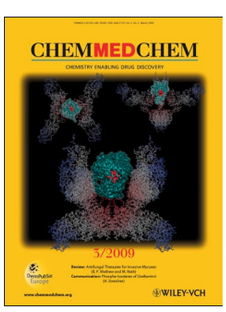

Autoimmunity

S. Wu, M. Bottini, R. C. Rickert, T. Mustelin, L. Tautz*

In Silico Screening for PTPN22 Inhibitors: Active Hits from an Inactive Phosphatase Conformation

2-Benzamidobenzoic acids seem to stabilize PTPN22 phosphatase in its inactive 'open' conformation with the WPD loop locked in a distal position. In silico screening using both 3D structures in open and closed conformations yielded potent inhibitors of this potential drug target for autoimmunity that specifically dock into its open form. Tryptophan fluorescence measurements support the proposed binding mode.

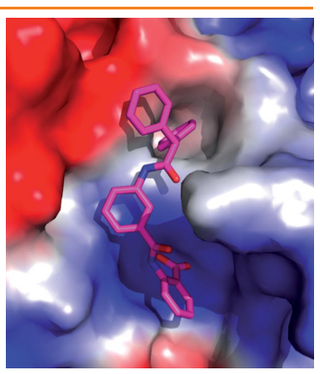

ChemMedChem
DOI: **10.1002/cmdc.200800375**

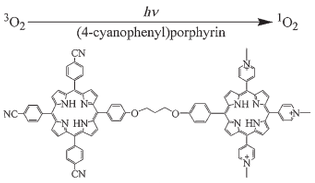

Eur. J. Inorg. Chem.
DOI: **10.1002/ejic.200801047**

Pd-Catalyzed Carbonylation

S. Yamashita, N. Kurono, H. Senboku, M. Tokuda, K. Orito*

Synthesis of Phenanthro[9,10-*b*]indolizidin-9-ones, Phenanthro[9,10-*b*]quinolizidin-9-one, and Related Benzolactams by Pd(OAc)$_2$-Catalyzed Direct Aromatic Carbonylation

Phenanthro[9,10-*b*]indolizidin-9-ones, phenanthro[9,10-*b*]quinolizidin-9-one, and related benzolactams were obtained by phosphane-free Pd(OAc)$_2$-catalyzed direct aromatic carbonylation from the corresponding amines. This constitutes a formal synthesis of the representative phenanthroindolizidine and -quinolizidine alkaloids (±)-tylophorine, (±)-antofine, and (±)-cryptopleurine.

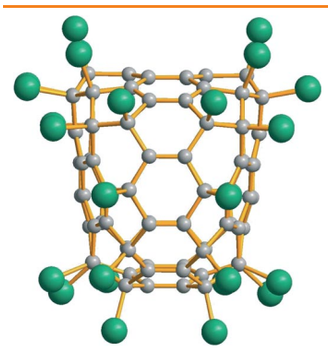

Angew. Chem. Int. Ed.
DOI: **10.1002/anie.200806332**

Halogenated Fullerenes

E. Kemnitz,* S. I. Troyanov*

Connectivity Patterns of Two C_{90} Isomers Provided by the Structure Elucidation of $C_{90}Cl_{32}$

Two for the price of one: The first halogenated derivative of C_{90}, $C_{90}Cl_{32}$ (see structure; gray C, green Cl), is obtained by chlorination of a higher fullerene mixture with $SbCl_5$. Its molecular structure, elucidated by single-crystal X-ray diffraction, reveals the presence of two isomeric C_{90} cages that correspond to C_{2v} isomer 46 and C_s isomer 34. The addition of 32 chlorine atoms is the maximum degree of chlorination achieved for fullerenes.

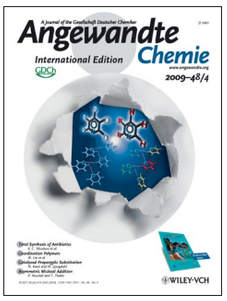

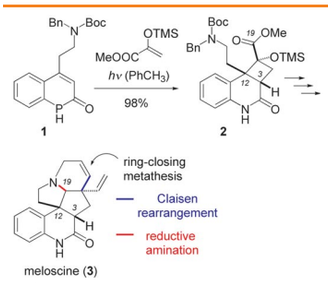

Chem. Eur. J.
DOI: **10.1002/chem.200802383**

Asymmetric Synthesis

P. Selig, E. Herdtweck, T. Bach*

Total Synthesis of Meloscine by a [2+2]-Photocycloaddition/Ring-Expansion Route

The stereogenic centers at C3 and C12 of meloscine (**3**) can be established in the photochemical key step **1** → **2**. 1,2-*Retro*-benzilic acid rearrangement to a five-membered ring, reductive amination, Claisen rearrangement, and ring-closing metathesis are further key steps in the transformation of cyclobutane **2** into the target molecule **3** (14 steps, 9% overall yield). Enantioselective access to (+)-meloscine was possible when the [2+2]-photocycloaddition was conducted in the presence of a chiral template.

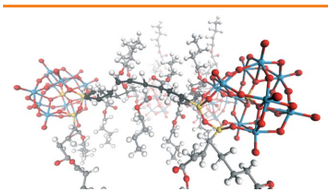

ChemSusChem
DOI: **10.1002/cssc.200800237**

Fuel Cell Membranes

J. L. Horan, A. Genupur, H. Ren, B. J. Sikora, M.-C. Kuo, F. Meng, S. F. Dec, G. M. Haugen, M. A. Yandrasits, S. J. Hamrock, M. H. Frey, A. M. Herring*

Copolymerization of Divinylsilyl-11-silicotungstic Acid with Butyl Acrylate and Hexanediol Diacrylate: Synthesis of a Highly Proton-Conductive Membrane for Fuel-Cell Applications

Highly conducive to high conductivity: Polyoxometalates were incorporated in the backbone of a hydrocarbon polymer to produce proton-conducting films. These first-generation materials contain large, dispersed clusters of polyoxometalates. Although the morphology of these films is not yet optimal, they already demonstrate practical proton conductivities and proton diffusion within the clusters appears to be very high.